Reactions $^{50}Cr(p,\gamma)^{51}Mn$ and $^{50}Cr(p,p'\gamma)^{50}Cr$ from 1.7 to 2.5 MeV

G. U. Din and A. M. AlSoraya
Van de Graaff Laboratory, Department of Physics, King Saud University, Riyadh, Saudi Arabia

J. A. Cameron, V. P. Janzen, and R. B. Schubank
Department of Physics, McMaster University, Hamilton, Ontario, Canada L8S 4K1

(Received 6 August 1985)

The yields of the (p,γ) and $(p,p'\gamma)$ reactions on ^{50}Cr were measured in the proton energy range 1.7 to 2.5 MeV with an energy resolution <2 keV. In all, 72 resonances were found, mostly in both channels. Nine resonances, at 1.936, 1.942, 2.030, 2.042, 2.113, 2.141, 2.187, 2.303, and 2.408 MeV were determined to be close multiplets. Gamma-ray spectra were measured at 53 resonances, including the multiplets. Angular distributions of the capture γ transitions at 40 resonances and of the $2^+\rightarrow 0^+$ γ transition in ^{50}Cr at 27 resonances were measured. The gamma decay schemes of the resonances provided information on 43 excited states of ^{51}Mn up to 5.174 MeV. Bound levels at 3.029, 3.835, 3.877, 3.955, 4.006, 4.046, and 4.153 MeV were populated for the first time in the (p,γ) reaction and their decay schemes were determined. Significant revisions of the decay schemes of the 2.276, 2.702, 2.893, 3.131, 3.292, 4.450, 4.540, 5.074, 5.129, and 5.174 MeV levels have resulted from the large number of resonances studied. Spins and parities for many resonances and bound states of ^{51}Mn have been determined from an extensive set of angular distribution measurements. In the proton energy range studied, 13 resonances are proposed as isobaric analogs of excited states from 2.704 to 3.207 MeV in ^{51}Cr.

I. INTRODUCTION

Levels of ^{51}Mn (Ref. 1) have been investigated by the proton transfer reactions (d,n), (^{3}He,d), (^{3}He,dγ), and (^{7}Li,^{6}He) on ^{50}Cr,[2-8] by the (p,α) and (p,$\alpha\gamma$) reactions on ^{54}Fe,[8-10] and the (^{16}O,p$\alpha\gamma$) and (^{14}N,n2pγ) reactions on ^{40}Ca.[9,11] There have also been several studies of resonances in the system $^{50}Cr + p$. The capture reaction has been studied below $E_p = 2.2$ MeV (Refs. 12–23) and at the $g_{9/2}$ isobaric analog resonances (3.1–3.4 MeV).[24] Elastic and inelastic scattering have been studied from 1.8 to 4.3 MeV (Refs. 25–31) and inelastic scattering to the first 2^+ and 4^+ levels of ^{50}Cr has recently been studied in the $g_{9/2}$ region.[32]

These studies have led to a well-developed level scheme of ^{51}Mn. Most of the levels can be accounted for within the context of a shell model in which only $f_{7/2}$ nucleons are active.[33] The lowest levels are predominantly $T=\frac{1}{2}$ while the $T=\frac{3}{2}$ levels, analogs of low ^{51}Cr states, appear as resonances in proton capture and scattering. In addition to the $f_{7/2}^{-5}$ states, there are a few levels of obviously different origin. A number of positive parity levels are known to exist in ^{51}Mn, the most certain of which is a $\frac{1}{2}^+$ state at 2.276 MeV (Refs. 3 and 5) and the $\frac{5}{2}^+$ and $\frac{9}{2}^+$ analog fragments above 8 MeV.[26,28,29,32] Other levels at low energy have been proposed as members of positive parity (presumably *sd* hole) bands, beginning at 1.817 MeV.[8] In ^{51}Cr, a number of low-lying levels, beginning with $\frac{3}{2}^-$ and $\frac{1}{2}^-$ isomers near 0.75 MeV, appear to be upper *fp*-shell intruder states. Because of the large number of degrees of freedom, shell model calculations capable of including these states must be restricted to one or two particles (holes) in one or two orbits above (below) $f_{7/2}$.

It was the intention of this study to extend the range of proton capture spectroscopy upward from 2 MeV, thereby to observe systematic trends in analog state properties with excitation energy and spin, and to obtain further spectroscopic information about the bound states. A brief report of part of this work has appeared elsewhere.[34]

II. EXPERIMENTAL

The measurements were made at the McMaster KN and King Saud AK Van de Graaff accelerators, using equipment and methods previously described.[32,34,35] The ^{50}Cr targets were evaporated onto degassed tungsten backings. The capture yield in $^{50}Cr + p$ is unusually low so particular care was taken in selecting target backings and aperture materials to minimize contamination, particularly by carbon and fluorine. Yield curves were measured in 1.1 keV steps from 1.7 to 2.5 MeV for a 20 μg/cm^2 target using a single HPGe detector close to the target at 55°. The inelastic channel was measured from the yield of the 0.783 MeV $2^+\rightarrow 0^+$ transition in ^{50}Cr and the capture channel from the yield of all γ rays with energy greater than 2 MeV. High resolution spectra ($\sim$6 keV FWHM at $E_\gamma = 7.5$ MeV) were obtained at the stronger resonances. Where resonances were suspected of being unresolved multiplets, a 10 μg/cm^2 target and 0.6 keV steps were used and spectra were obtained at each step. The accelerator energy calibration was checked using the capture γ-ray energies at strong resonances and an aluminum target at the 0.992 MeV resonance. The latter was also used, along with calibrated sources, to measure the energy dependence of the efficiency of the detectors.

For the angular distributions, the detector was with-

TABLE I. Resonances in $^{50}Cr + p$, $1.7 \leq E_p \leq 2.5$ MeV. s represents spectrum observed, w represents weak resonance.

Resonance No.	E_p (MeV)		E_x (MeV)	Intensity (p,γ)	Intensity (p,p'γ)	J^π a	J^π Other
1	1.798	s	7.034	2204	411	$\frac{3}{2}^-$	$\frac{3}{2}^-$ [b]
2	1.803		7.038	167			
3	1.810	s	7.045	987		$\frac{1}{2}$	$\frac{1}{2}^+$ [c]
4	1.819		7.045	146			
5	1.830	s	7.065	2856	476	$\frac{3}{2}^-$	$\frac{3}{2}^-$ [b]
6	1.861		7.095	215			
7	1.872	s	7.106	1575	146	$\frac{5}{2}, \frac{7}{2}^-$	
8	1.878		7.112	480	192		
9	1.895	s	7.129	2379	872	$\frac{1}{2}$	$\frac{1}{2}^-$ [c,d]
10	1.902		7.136	265			
11	1.908	s	7.141	1374	100	$\frac{5}{2}^-$	
12	1.913	s	7.146	1264	109	$\frac{3}{2}^-$	
13	1.929	s	7.162	3392	212	$\frac{1}{2}^-$	
14a	1.936	s	7.169	2149	1220	$\frac{1}{2}^-$	
14b	1.937		7.170			$\frac{5}{2}^-$	
15a	1.942	s	7.175	3690		$\frac{5}{2}$	
15b	1.943		7.176			$\frac{5}{2}^+$	$\frac{1}{2}^+$ [c]
16	1.958	s	7.190	1685	1404	$\frac{3}{2}^-$	$\frac{1}{2}^-$ [c,d]
17	1.972		7.204	370			
18	1.978	s	7.210	590	w	$(\frac{5}{2})$	
19	1.981	s	7.213	489	w	$(\frac{1}{2}, \frac{3}{2})$	
20	1.990	s	7.222	608	274	$\frac{5}{2}^-$	
21	1.995		7.227	688			
22	2.009	s	7.240	1316		$\frac{5}{2}^{(+)}$	
23a	2.030	s	7.261	2767	259	$\frac{5}{2}^-$	
23b	2.030		7.261			$\frac{1}{2}$	$\frac{1}{2}^+$ [c]
24a	2.042	s	7.273	4599	1949	$\frac{5}{2}$	$\frac{5}{2}$ [e]
24b	2.043		7.274			$\frac{3}{2}^-$	$\frac{3}{2}^-$ [c,d]
25	2.066	s	7.296	3831	965	$\frac{3}{2}^-$	$\frac{3}{2}^-$ [d]
26	2.074		7.304	398			
27	2.080	s	7.310	750	2575	$\frac{5}{2}^+$	
28	2.084	s	7.314	411		$(\frac{1}{2})$	
29	2.110	s	7.339	w	w	$(\frac{1}{2})$	
30a	2.113	s	7.342	4855	2400	$\frac{3}{2}^+$	
30b	2.114		7.343			$\frac{3}{2}^-, \frac{5}{2}^-$	$\frac{3}{2}^-$ [c,d]
31	2.128	s	7.357	1829		$\frac{5}{2}^-$	
32a	2.141	s	7.370	7669	2060	$\frac{3}{2}^+, \frac{5}{2}^-$	
32b	2.142		7.371			$\frac{3}{2}^-$	$\frac{3}{2}^-$ [c,d]
33	2.158		7.386	w	w		
34	2.161		7.389	622	195		
35	2.167	s	7.395	1243	600	$\frac{3}{2}^-, \frac{5}{2}^-$	$\frac{3}{2}^-$ [c]
36	2.182		7.410				$\frac{1}{2}^+$ [c]

TABLE I. (*Continued*).

Resonance No.	E_p (MeV)		E_x (MeV)	Intensity (p,γ)	Intensity (p,p'γ)	J^π a	J^π Other
37*a*	2.187	*s*	7.415	1803	890	$\frac{5}{2}^+$	
37*b*	2.187		7.415			$\frac{3}{2}^-$	
38	2.199		7.427	624			
39	2.206		7.434	220			$\frac{1}{2}^+$ [c]
40	2.220	*s*	7.447	1531	350	$\frac{3}{2}^-$	
41	2.223	*s*	7.450	2365	540	$\frac{3}{2}^-$	
42	2.232	*s*	7.459	1021	860	$\frac{5}{2}^+$	
43	2.236	*s*	7.463	510		$(\frac{5}{2}, \frac{7}{2})$	
44	2.240	*s*	7.467	1680		$\frac{1}{2}^-$	$\frac{1}{2}^-$ [c]
45	2.250		7.477	*w*	*w*		
46	2.255		7.482	*w*	419		
47	2.257		7.484	*w*			
48	2.275		7.501	274	901	$\frac{5}{2}^+$	
49	2.288	*s*	7.514	899		$\frac{5}{2}^-$	
50	2.293		7.519	440			
51	2.299		7.525	826			$\frac{1}{2}^+$ [c]
52*a*	2.303	*s*	7.529	5152	2700	$\frac{3}{2}^-, \frac{5}{2}^-$	$\frac{3}{2}^-$ [d]
52*b*	2.304		7.530				
53	2.321	*s*	7.546	1710	9000	$\frac{5}{2}$	
54	2.325	*s*	7.550	4820		$\frac{1}{2}^-$	$\frac{1}{2}^-$ [c,d]
55	2.335	*s*	7.560	6637	16 500	$\frac{3}{2}^-, \frac{5}{2}^-$	$\frac{3}{2}^-$ [c,d]
56	2.347	*s*	7.572	1130	26 260	$\frac{5}{2}^+$	$(\frac{5}{2}^+)$ [c]
57	2.355		7.580	*w*			
58	2.362	*s*	7.586	1063		$(\frac{1}{2}, \frac{3}{2})$	$\frac{1}{2}$ [c,d]
59	2.375	*s*	7.599	580		$(\frac{3}{2})$	
60	2.390		7.614	*w*			
61	2.394	*s*	7.618	510		$\frac{1}{2}$	
62	2.397	*s*	7.621	700		$\frac{9}{2}^+$	
63*a*	2.407	*s*	7.631	1795	1193	$\frac{5}{2}^-$	
63*b*	2.408		7.632			$\frac{5}{2}^+$	
64	2.412	*s*	7.636	338	1276	$\frac{5}{2}^+$	
65	2.420		7.643	1133		$(\frac{1}{2}, \frac{3}{2})$	$\frac{1}{2}^-$ [c,d]
66	2.433		7.656	*w*	*w*		
67	2.446	*s*	7.669	1607	*w*	$(\frac{5}{2}, \frac{7}{2})$	
68	2.455		7.678		*w*		
69	2.461	*s*	7.684	934	6727	$(\frac{3}{2})$	$\frac{3}{2}^-$ [c,d]
70	2.465		7.687	1208			
71	2.477	*s*	7.699	2189	5389	$\frac{5}{2}^+$	
72	2.500	*s*	7.722	1190	19 000	$\frac{3}{2}^-$	$\frac{3}{2}^-$ [c,d]

[a] Present work.
[b] Reference 16.
[c] Reference 26.
[d] Reference 27.
[e] Reference 22.

drawn to 10 cm from the target and another similar detector was placed as a monitor at $-90°$. Distributions, measured at 0°, 30°, 45°, 60°, and 90°, were analyzed at the 0.783 MeV (p,p'γ) peak according to the prescription used in Ref. 32. The ratio of the $2^+ \rightarrow 0^+$ γ-ray intensity in the moving detector to that in the fixed detector was fitted in the first instance for a single resonance spin, allowing mixtures of different exit channel angular momenta where appropriate. When no good fit was possible for a single resonance spin, pairs of spins (unresolved doublets) were considered. The angular distributions of capture transitions were also obtained where the intensity permitted and analyzed as in Ref. 35. In this case, normalization was made whenever possible to isotropic capture cascade transitions such as that at 1.959 MeV ($\frac{1}{2}^- \rightarrow \frac{5}{2}^-$) seen in the moving detector. Strong capture lines and the (p,p'γ) transition observed in the fixed detector were used when the internal normalization was not possible. In the determination of the resonance spins and parities, only capture transitions to states whose J^π values are well established[1,3,5,7,9] were used. These are $(E_x, J^\pi) = (0, \frac{5}{2}^-)$, $(0.237, \frac{7}{2}^-)$, $(1.140, \frac{9}{2}^-)$, $(1.825, \frac{3}{2}^-)$, $(1.959, \frac{1}{2}^-)$, $(2.140, \frac{3}{2}^-)$, $(2.256, \frac{5}{2}^-)$, $(2.276, \frac{1}{2}^+)$, $(2.416, \frac{7}{2}^-)$, and $(2.914, \frac{3}{2}^-)$. For each choice of resonance spin, the value of the $E2/M1$ mixing ratio δ (phase convention of Rose and Brink[36]) giving the best fit was found. Values of resonance spin for which a minimum χ^2 greater than 5 was found were rejected. Where the fit required a quadrupole-to-dipole intensity ratio δ^2 greater than 5%, the transition was taken to have even parity, so $\pi_i = \pi_f$. The assignment of spin-$\frac{1}{2}$ from isotropic distributions was made uniquely only when several such distributions originated from a single resonance, according to the criterion suggested by van der Leun and Nooren.[37] With established values of J^π for resonances, it was possible to use a similar procedure to deduce spin-parity values for a number of bound states of ^{51}Mn. In some cases, γ-ray intensities were not sufficient to allow angular distribution measurements to be made. Where spectra were obtained, the spins of resonances and bound states were inferred assuming only dipole and electric quadrupole transitions. These appear in parentheses in Tables I and V.

III. RESULTS

A. Excitation functions

The inelastic and capture yields measured at 55° are shown, respectively, in parts (a) and (b) of Figs. 1 and 2. In all, some 72 peaks are discernible. They are listed in

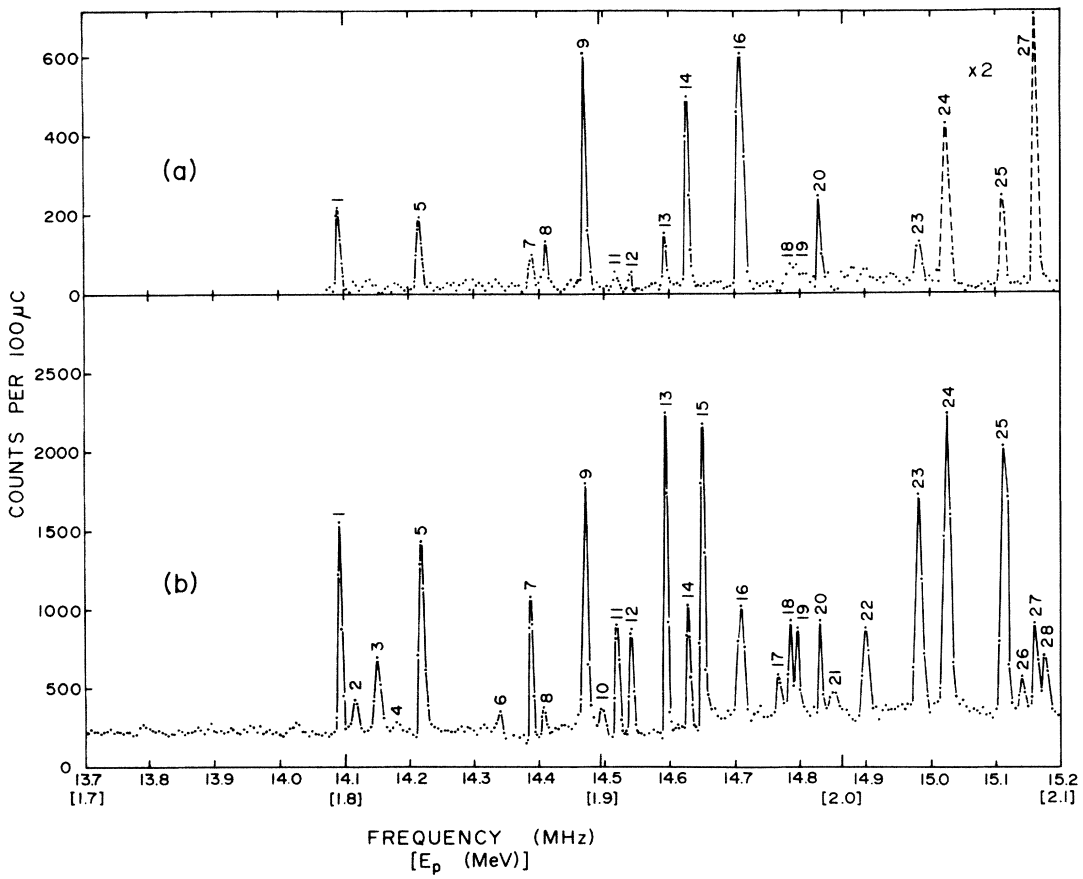

FIG. 1. Yields of the reactions (a) ^{50}Cr(p,p'γ)^{50}Cr and (b) ^{50}Cr(p,γ)^{51}Mn from 1.7 to 2.1 MeV, measured at 55°. The inelastic yield was measured from the 0.783 MeV $2^+ \rightarrow 0^+$ transition in ^{50}Cr while the capture yield included all γ rays with energies greater than 2 MeV. The peaks are numbered sequentially and further identified in Table I. The scale of proton bombarding energies is shown in brackets. The dashed curves indicate regions of altered ordinate scale.

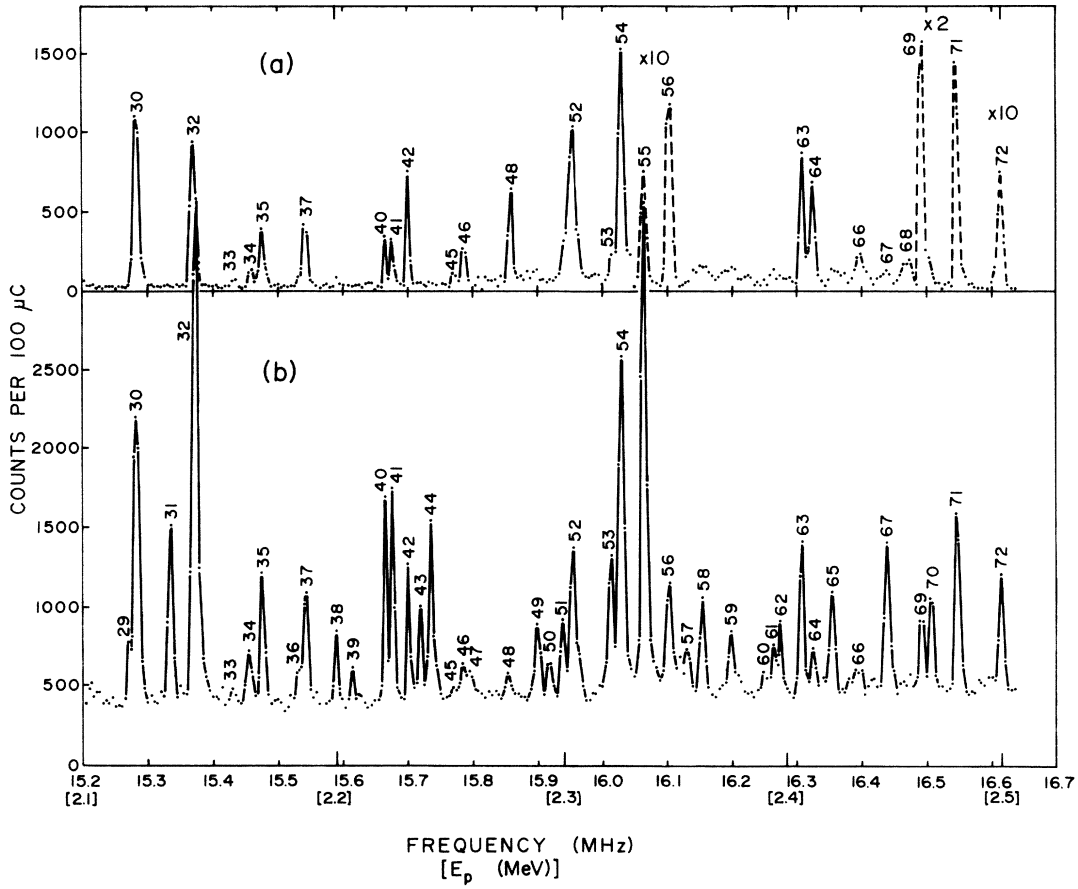

FIG. 2. Yield from 2.1 to 2.5 MeV. Details as in Fig. 1.

Table I where E_p, E_x, and intensities of the capture region of the spectrum and of the inelastic peak are given. Of all the (p,p'γ) peaks only one, No. 68 at 2.455 MeV, fails to appear in the (p,γ) yield. On the other hand, many peaks seen in (p,γ) are missing from the inelastic yield. The overall resolution is 1.5—2 keV and the reproducibility was about 1 keV from one scan to another.

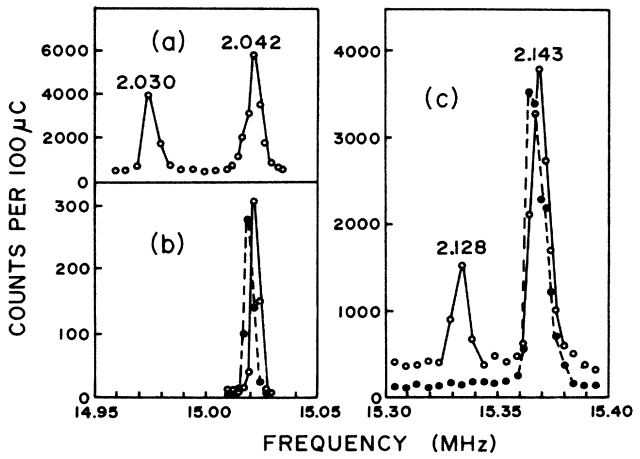

FIG. 3. Detailed yield curves in the regions of two close doublet resonances. (a) No. 24, at 2.043 MeV: integral yield of the (p,γ) reaction; (b) the same, yields to the ground ($\frac{5}{2}^-$) and first excited ($\frac{7}{2}^-$) states are shown by the solid and dashed curves, respectively; (c) No. 32, at 2.143 MeV: the solid and dashed curves show the integral (p,γ) and the (p,p'γ) yields.

There are a number of incompletely resolved peaks whose multiplet nature was revealed by measuring the yields of individual capture branches from the resonance. An example (resonance Nos. 61 and 62) is given in detail in Ref. 34. Two others, shown in Fig. 3, are detailed yield curves at the 2.042 and 2.143 MeV resonances, Nos. 24 and 32, respectively. For the former, the integral capture yield is compared to that for transitions to the ground and first excited states of ^{51}Mn, while for the latter the integral capture yield and inelastic yield are compared. In all, nine resonances, Nos. 14, 15, 23, 24, 30, 32, 37, 52, and 63, proved to be closely spaced doublets.

B. Decay schemes of resonances

Gamma-ray spectra were measured for the 53 resonances marked "*s*" in Table I, including the nine close doublets. A typical spectrum, at resonance No. 31, $E_p=2.128$ MeV, is shown in Fig. 4. In addition to the capture primary and cascade γ rays in ^{51}Mn and the strong inelastic γ rays from ^{50}Cr at 0.783 MeV and ^{183}W at 0.291 MeV, there are a number of impurity lines from $^{19}F(p,\alpha\gamma)^{16}O$ and $^{23}Na(p,\alpha\gamma)^{20}F$ as well as (p,p'γ) reactions on ^{23}Na and ^{27}Al. The proton beam energy resolution and stability over a number of hours made it possible to accumulate spectra for each side of doublet peaks.

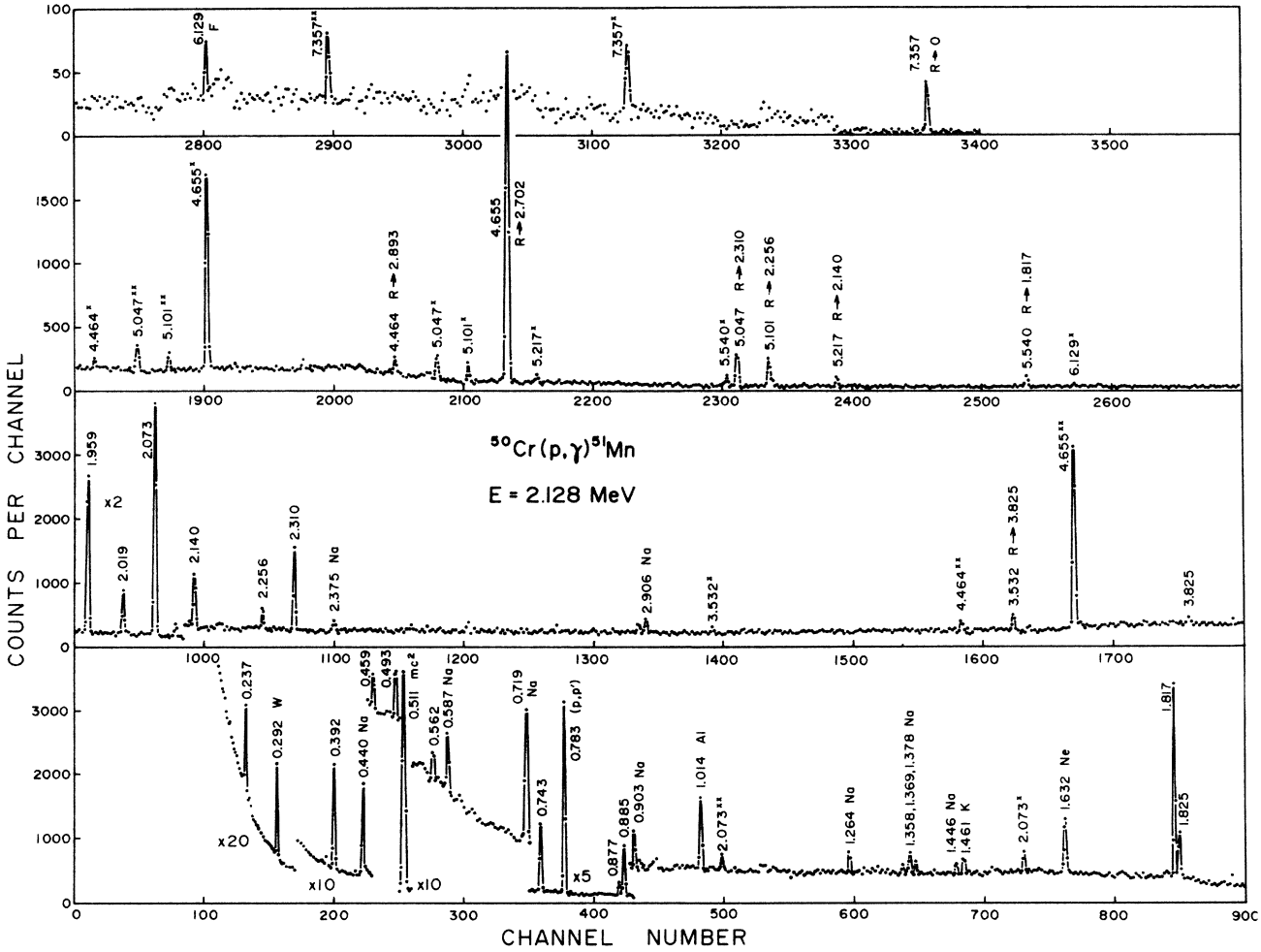

FIG. 4. Spectrum of γ rays at the 2.128 MeV resonance, No. 31.

TABLE II. Decay branching from $^{50}Cr(p,\gamma)^{51}Mn$ resonances.

Resonance No. E_f (MeV)	1	3	5	7	9	11	12	13	14*a*	14*b*	15*a*	15*b*	16	18
0.0	17		41	11		3	7	64	2	7	29		20	
0.237				18		42	7			41	24		2	
1.140						7								
1.488														
1.817		15		10			10					18		
1.825	15		36		9			3	4	11			11	22
1.959	40				69		46	3	44				4	
2.140	6	20			18			3	11	30		10	20	32
2.256						19		5						
2.276		65									18			
2.310				39				6			5			
2.416						8					5			39
2.702				5							8		4	
2.841								3	3					
2.893				10								22		
2.914	6			7	3		12	2	16		33			
2.985														
3.029														
3.049														
3.131			5								1			
3.292			4										10	

TABLE II. (*Continued*).

Resonance No. E_f (MeV)	1	3	5	7	9	11	12	13	14*a*	14*b*	15*a*	15*b*	16	18
3.423						9								
3.554	4		2					5	4	11				
3.694			4											
3.825											4			
3.835														
3.877														
3.893	11		8			5			8					
3.955														
4.006														
4.046												5		
4.153						2						9		
4.200								3	3					
4.206							13							
4.358	1				1	5	5		5					
4.450												9		
4.488														
4.540													7	1
4.723								1						
4.883														
4.923								2						
5.074													11	
5.129													15	
5.174													3	

Resonance No. E_f (MeV)	19	20	22	23	24*a*	24*b*	25	27	28	29	30	31
0.0		65	24	1		23	10				20	4
0.237			18	7	76			6				
1.140												
1.488												
1.817	17		4	17			1	31		18		6
1.825			6	6		10	6		18		16	
1.959				10		10	34		20		2	
2.140				12		12	3		35		4	2
2.256						5	22	5			2	7
2.276	30		2	1						82		
2.310				3	20			13				6
2.416			2	1				4				
2.702				19		4						69
2.841						6			16		4	
2.893				3								3
2.914	16		4	1				8			20	
2.985		35				18	7	14			20	
3.029												
3.049												
3.131				9								
3.292			18								4	
3.423			8									
3.554							3					
3.694						2			11		4	
3.825								10				3
3.835												
3.877												
3.893			7			5					4	
3.955												
4.006			7									
4.046				5								
4.153								9				
4.200	25											

TABLE II. (*Continued*).

Resonance No. E_f (MeV)	19	20	22	23	24*a*	24*b*	25	27	28	29	30	31
4.206						5						
4.358	12											
4.450				3								
4.488							6					
4.540				2	4							
4.723												
4.883							6					
4.923												
5.074												
5.129												
5.174							2					

Resonance No. E_f (MeV)	32*a*	32*b*	35	37	40	41	42	43	44	49	52	53
0.0		19	38	8	6	10	8	53	10		18	39
0.237				7		2	5	47		44	2	53
1.140												
1.488												
1.817				10	41				31	5		
1.825	26	17		6		15	14				11	
1.959				15					4			
2.140		13		6		53			4	20	11	
2.256						3	3				19	
2.276		6			25				4			
2.310	23			21	18	3	6			16	5	6
2.416				9			11					
2.702				4			27				3	
2.841						5					9	
2.893				2			16					
2.914		20		2					38		3	
2.985	43	23				3						
3.029												
3.049	8									8		
3.131					10		10					
3.292		9	62								6	2
3.423												
3.554				1							7	
3.694									6			
3.825				7						6		
3.835												
3.877												
3.893		5		1					2		2	
3.955												
4.006										1		
4.046												
4.153												
4.200												
4.206		2										
4.358		2				2					2	
4.450												
4.488						4						
4.540				1								
5.723		1										
4.883									1			
4.923												
5.074		2										
5.129											2	
5.174												

TABLE II. (*Continued*).

Resonance No. E_f (MeV)	54	55	56	58	59	61	62	63	64	65	67	69	71	72
0.0	1	7	2		14			11	32		38	11	48	9
0.237		9	13				23	31	16		62		27	
1.140							45							
1.488							8							
1.817						70		3					11	
1.825	16	4	16	13	58					25				15
1.959	4	2			28	10				21		13		43
2.140	27	27	8	7				10		20		19		
2.256		14											3	
2.276			19			20								
2.310							11	9					8	
2.416								7	15					
2.702	3	1	22										3	16
2.841		2		37								19		5
2.893														
2.914	40			31										
2.985										15		18		6
3.029							6							
3.049								15						
3.131		1						8	37					
3.292		18										8		
3.423								2						
3.554	3											12		
3.694	3													
3.825			7					2						
3.835							5							
3.877								2						
3.893	3	3		9										
3.955							2							
4.006		7												
4.046														
4.153														
4.197														
4.206		2		3										4
4.358														
4.450			5											
4.488		3												2
4.540														
4.723														
4.883														
4.923														
5.074														
5.129			8											
5.174									19					

There was good separation of γ-ray spectra from one member of the doublets to the other even when the two components were separated by only 1 keV. For example, resonance 15*a* at 1.942 MeV populates nine bound levels while its partner 15*b* at 1.943 MeV populates six quite different levels. In all, 43 bound levels were populated up to an excitation energy of 5.175 MeV. The estimated absolute uncertainties in the branching ratios given in Table II are about 1% at most of the resonances studied. The study of a large number of resonances made it possible to determine the decay schemes of each of the bound levels from several strong feeding resonances. The energies of the 43 excited states found in the decay of resonances and the branching ratios of the secondary transitions are given in Table III, where generally the values given are averages for several resonances. For comparison, corresponding data from previous studies are given. The bound levels at 3.029, 3.825, 3.835, 3.877, 3.955, and 4.200 MeV were populated for the first time in the (p,γ) reaction.

C. Angular distributions

Typical angular distributions are illustrated in Fig. 5, for resonance No. 49, at $E_p = 2.288$ MeV. The $(p,p\gamma)$ dis-

TABLE III. Gamma-ray branching ratios in ^{51}Mn.

Transition	E_γ (MeV)	Branching ratios a	b	c	d
0.237→0	0.237	100	100	100	100
1.140→0	1.140	15	11	14	10
0.237	0.903	85	89	86	90
1.488→0	1.488			<2	
0.237	1.251			64	
1.140	0.348			36	
1.817→0	1.817	100	100	97	100
0.237	1.580			3	
1.825→0	1.825	100	100		100
1.959→0	1.959	100	100	>98	100
0.237	0.722			<2	
2.140→0	2.140	100	100	98	100
0.237	1.903			2	
2.256→0	2.256	27	31		20
0.237	2.019	73	69		80
2.276→0	2.276	2			
1.817	0.459	61	70	78	70
1.825	0.451	11			
1.959	0.317	12	30	22	30
2.140	0.136	14			
2.310→0	2.310	11	19	15	15
0.237	2.073	79	81	85	85
1.817	0.493	10			
2.416→0	2.416		10	<5	6
0.237	2.179	57	48	60	34
1.140	1.276	43	42	40	37
1.817	0.599				15
2.140	0.170				8
2.702→1.140	1.562				2
1.817	0.885	19		23	21
1.825	0.877	7			
1.959	0.743	28	38	33	26
2.140	0.562	4			
2.276	0.426	4			
2.310	0.392	38	62	44	37
2.841→1.825	1.016	45	25		40
1.959	0.882	55	75	>70	60
2.893→0	2.893	36	38		35
0.237	2.656	6			
1.140	1.753	35	37		45
1.817	1.076	20	25		20
1.825	1.068	3			
2.914→0	2.914	100	100	100	100
2.985→0	2.985	29	30	31	20
0.237	2.748	71	70	69	80

TABLE III. (*Continued*).

Transition	E_γ (MeV)	Branching ratios a	b	c	d
3.029→0	3.029	37			
0.237	2.792	63			
3.049→0.237	2.812	46	25		
1.140	1.909	28			
1.817	1.232	26			40
2.256	0.793		33		45
2.276	0.773		13		15
3.131→1.817	1.314	56	47		45
1.825	1.305	15			
2.140	0.991	19	9		
2.256	0.875				12
2.276	0.855		4		
2.310	0.821	10	10		
3.293→0	3.293	27	33		35
0.237	3.056	60	47		65
2.140	0.991	3	20		
2.256	1.037	10			
3.426→0	3.426	100	75		
1.959	1.467		25		100
3.554→0	3.554	100	100		100
3.694→0	3.694	38	15		20
1.825	1.869	37	50		55
2.140	1.554	25	25		25
2.914	0.780		10		
3.825→0	3.825	59			
0.237	3.589	12			
1.140	2.685	29			
3.834→1.140	2.685	25			
2.256	1.569	45			
?		30			
3.877→1.959	1.918	50			
?		50			
3.893→0	3.893	100	97		100
2.841	1.052		3		
3.955→1.140	2.815	28			
?		72			
4.006→0.237	3.769	68			
2.276	1.730	32			
4.046→0	4.046	100			
4.153→1.825	2.328	67			
2.140	2.013	33			
4.200→1.817	2.383	60			
2.276	1.924	40			
4.205→0	4.205	27	33		20
0.237	3.968	43	34		20

TABLE III. (*Continued*).

Transition	E_γ (MeV)	Branching ratios a	b	c	d
1.817	2.388	15			
1.825	2.380	15	33		60
4.358→0	4.358	100	100		45
1.959	2.399				20
3.555	0.803				35
4.450→1.817	2.633	36			
1.825	2.625		46		45
1.959	2.491				20
2.256	2.194	34			
2.310	2.140				35
3.131	1.319	30			
4.488→0.237	4.251	63	100		
2.256	2.232	37			
4.540→1.959	2.581	50			
2.702	1.838	50			
1.140	3.400		100		
4.723→0	4.723				85
2.702	2.021	100			
4.883→1.959	2.924	50	70		13
2.140	2.743	50			
2.841	2.042				60
4.923→2.310	2.613	55			
2.914	2.009				75
2.985	1.938				25
?		45			
5.074→1.817	3.257				15
1.959	3.115	40			35
2.256	2.818	60			
2.276	2.798				50
5.129→1.817	3.312	23			
1.825	3.304	15			
2.256	2.873	40			
2.310	2.819	22			75
2.985	2.144				25
5.175→1.825	3.350	48			100
1.959	3.216	52			

[a]Present work.
[b]Reference 19.
[c]Reference 9.
[d]Reference 22.

tribution is shown in Fig. 5(a) with fits for a number of spin choices. Figures 5(b) and (c) show the distributions for capture transitions to two bound levels of known spin and parity, together with the corresponding plots of χ^2 vs $\tan^{-1}\delta$. Clearly the capture data select $J_R = \frac{5}{2}$. The small mixing ratios in the decays prevent a parity assignment. However, the inelastic fit requires negative parity (mixed $j_{p'} = \frac{1}{2}$ and $\frac{3}{2}$ in the inelastic exit channel). In Fig. 5(d), the distribution for capture to a state of unknown J^π is shown with its analysis. The data eliminate spin $\frac{1}{2}$ but allow $\frac{3}{2}$, $\frac{5}{2}$, and $\frac{7}{2}$, all with appreciable mixing, implying negative parity. Table IV contains a summary of the angular distribution data for 35 resonances, with the spin-parity options allowed. The notation "1,2" in the mul-

TABLE IV. Angular distributions in $^{50}Cr(p,p'\gamma)^{50}Cr$ and $^{50}Cr(p,\gamma)^{51}Mn$.

Resonance No.	E_i (MeV)	E_f (MeV)	A_2	A_4	J_i^π	J_f^π	Multipolarity	χ^2
1		inel.	0.40(4)	−0.04(4)	$\frac{3}{2}, \frac{5}{2}^-$			
	7.034	0.0	−0.15(4)	−0.09(4)	$\frac{3}{2}^-$	$\frac{5}{2}^-$	1,2	1.5
		1.959	−0.23(5)	0.04(5)		$\frac{1}{2}^-$	1,2	1
3	7.045	1.817	−0.01(6)	0.02(7)	$\frac{1}{2}$	$\frac{3}{2}$		0.1
		2.140	−0.12(6)	−0.02(7)		$\frac{3}{2}^-$		4
		2.276	0.05(4)	0.01(4)		$\frac{1}{2}^+$		2
5		inel.	0.13(4)	−0.06(5)	$\frac{3}{2}^-$			
7	7.106	0.0	0.47(6)	−0.09(6)	$\frac{5}{2}$	$\frac{5}{2}^-$	1	1.5
					$\frac{7}{2}^-$		1,2	3
		0.237	−0.22(6)	0.03(6)	$\frac{5}{2}$	$\frac{7}{2}^-$	1	0.2
					$\frac{7}{2}^-$		1,2	1
9		inel.	0.02(2)	0.01(2)	$\frac{1}{2}$			
	7.129	1.825	0.04(5)	−0.02(2)	$\frac{1}{2}$	$\frac{3}{2}$		2
		1.959	0.02(2)	−0.02(2)		$\frac{1}{2}^-$		1
		2.140	0.05(4)	−0.05(5)		$\frac{3}{2}^-$		4
11	7.141	0.237	−0.48(4)	−0.08(4)	$\frac{5}{2}^-$	$\frac{7}{2}^-$	1,2	2
		2.256	0.80(5)	−0.23(5)		$\frac{5}{2}^-$	1,2	4
12	7.146	1.959	0.17(4)	−0.03(4)	$\frac{3}{2}^-$	$\frac{1}{2}^-$	1,2	1.5
		2.914	0.10(5)	−0.01(5)		$\frac{3}{2}^-$	1	0.2
13		inel.	0.08(3)	−0.03(3)	$\frac{1}{2}$			
	7.162	0.0	−0.06(1)	0.03(1)	$\frac{1}{2}^-$	$\frac{5}{2}^-$		4
		1.959	0.03(2)	0.02(2)		$\frac{1}{2}^-$		1
14*a*		inel.	0.01(2)	−0.01(2)	$\frac{1}{2}$			
	7.169	0.0	−0.09(5)	0.16(6)	$\frac{1}{2}^-$	$\frac{5}{2}^-$		5
		1.959	0.04(4)	0.00(4)		$\frac{1}{2}^-$		0.1
		2.140	0.01(6)	−0.07(6)		$\frac{3}{2}^-$		2.5
14*b*	7.170	0.237	−0.51(6)	0.02(6)	$\frac{5}{2}^-$	$\frac{7}{2}^-$	1,2	0.1
15*a*	7.175	0.0	0.51(3)	−0.17(3)	$\frac{5}{2}^-$	$\frac{5}{2}^-$	1,2	2
		0.237	−0.04(3)	−0.13(2)		$\frac{7}{2}^-$	1	5

TABLE IV. (*Continued*).

Resonance No.	E_i (MeV)	E_f (MeV)	A_2	A_4	J_i^π	J_f^π	Multipolarity	χ^2
15*b*	7.176	2.140	0.07(5)	−0.20(5)	$\frac{1}{2}$	$\frac{3}{2}^-$		4
		2.893	0.09(3)	−0.07(3)		$\frac{3}{2}, \frac{5}{2}$		5
16	inel.		0.25(2)	−0.08(2)	$\frac{3}{2}^-, \frac{5}{2}^-$			
	7.190	2.140	0.82(5)	0.32(6)	$\frac{5}{2}^-$	$\frac{3}{2}^-$	1,2	2
20	inel.		0.50(4)	−0.14(5)	$\frac{5}{2}^-$			
22	7.240	0.0	0.55(6)	−0.16(7)	$\frac{5}{2}^-$	$\frac{5}{2}$	1	2
23*a*	7.261	0.0	0.11(10)	−0.02(11)	$\frac{5}{2}^-$	$\frac{5}{2}^-$	1,2	0.4
		0.237	−0.10(2)	0.04(2)		$\frac{7}{2}^-$	1	1
		2.702	−0.11(2)	0.11(2)		$\frac{3}{2}^-$	1,2	6
		3.131	0.36(3)	−0.01(4)		$\frac{7}{2}^-$	1,2	1.5
23*b*	7.262	1.959	−0.01(3)	0.09(3)	$\frac{1}{2}$	$\frac{1}{2}^-$		4
		2.140	−0.02(3)	0.05(3)		$\frac{3}{2}^-$		1
24*a*	7.273	0.237	−0.17(2)	0.08(2)	$\frac{5}{2}^-$	$\frac{7}{2}^-$	1,2	2
		2.310	0.16(4)	0.00(4)		$\frac{5}{2}^-$	1,2	2
24*b*	7.274	0.0	−0.35(2)	0.00(2)	$\frac{3}{2}^-$	$\frac{5}{2}^-$	1,2	1
		1.825	0.43(3)	0.04(3)		$\frac{3}{2}^-$	1	0.7
		1.959	−0.57(3)	0.01(3)		$\frac{1}{2}^-$	1	0.3
		2.841	−0.68(7)	0.03(3)		$\frac{1}{2}, \frac{3}{3}, \frac{5}{2}$	1,2	1
		2.985	−0.03(3)	−0.03(3)		$\frac{1}{2}^-, \frac{3}{2}^-$	1,2	1
		3.694	0.14(11)	−0.01(11)		$\frac{1}{2}, \frac{3}{2}, \frac{5}{2}$	1,2	0.1
		3.893	0.32(5)	0.08(6)		$\frac{1}{2}^-, \frac{5}{3}^-$	1,2	2
						$-\frac{3}{2}$	1	2
25	inel.		0.50(2)	−0.07(2)	$\frac{3}{2}, \frac{5}{2}^-$			
	7.296	0.0	0.39(4)	−0.05(4)	$\frac{3}{2}^-$	$\frac{5}{2}^-$	1,2	4
		1.959	0.36(2)	0.06(2)		$\frac{1}{2}^-$	1	3
		2.256	−0.10(3)	0.03(3)		$\frac{5}{2}^-$	1	0.8
		2.985	−0.03(7)	0.01(8)		$\frac{5}{2}^-$	1	6
		4.883	−0.44(12)	−0.13(11)		$\frac{1}{2}, \frac{3}{2}^-, \frac{5}{2}^-$	1,2	0.6
27	inel.		0.51(2)	−0.54(2)	$\frac{5}{2}^+$			
	7.310	3.825	0.11(5)	0.13(6)	$\frac{5}{2}$	$\frac{3}{2}, \frac{5}{2}$	1,2	2
						$\frac{7}{2}$	1	2

TABLE IV. (*Continued*).

Resonance No.	E_i (MeV)	E_f (MeV)	A_2	A_4	J_i^π	J_f^π	Multipolarity	χ^2
30*a*	inel.		0.47(2)	−0.06(2)	$\frac{3}{2}^+, \frac{5}{2}^-$			
	7.342	2.276	−0.13(4)	−0.08(4)	$\frac{3}{2}^+$	$\frac{1}{2}^+$	1,2	4
30*b*	7.342	0.0	0.09(3)	0.01(4)	$\frac{3}{2}^-$	$\frac{5}{2}^-$	1,2	0.1
		1.825	0.32(3)	0.02(4)		$\frac{3}{2}^-$	1	0.4
		2.140	0.27(11)	0.19(12)		$\frac{3}{2}^-$	1	3
		2.983	0.01(2)	−0.09(2)		$\frac{5}{2}$	1	10
31	7.357	0.0	0.70(10)	0.03(10)	$\frac{5}{2}^-$	$\frac{5}{2}^-$	1,2	0.5
		1.817	0.62(9)	0.27(7)		$\frac{3}{2}$	1	4
		2.256	0.63(11)	0.07(11)		$\frac{5}{2}^-$	1,2	1
		2.310	0.59(7)	0.03(7)		$\frac{5}{2}^-$	1,2	0.4
		2.702	−0.24(3)	0.07(3)		$\frac{3}{2}^-$	1	4
32*a*	inel.		0.35(2)	0.06(2)	$\frac{3}{2}^-, \frac{5}{2}^-$			
	7.370	1.825	0.13(1)	0.04(2)	$\frac{3}{2}^-$	$\frac{3}{2}^-$	1,2	6
		2.985	0.20(2)	0.00(2)		$\frac{5}{2}^-$	1,2	1
32*b*	7.371	0.0	0.05(3)	0.02(2)	$\frac{3}{2}^-$	$\frac{5}{2}^-$	1	0.3
		2.140	0.31(2)	0.07(3)		$\frac{3}{2}^-$	1	5
		2.914	0.41(2)	0.02(3)		$\frac{3}{2}^-$	1	1
		3.292	−0.04(5)	−0.06(6)		$\frac{1}{2}^-, \frac{3}{2}^-$	1,2	2
						$\frac{5}{2}$	1	1.5
34	inel.		0.40(6)	0.06(7)	$\frac{3}{2}^-, \frac{5}{2}^-$			
35	inel.		0.34(3)	−0.03(3)	$\frac{3}{2}^-, \frac{5}{2}^-$			
37*a*	inel.		0.30(2)	−0.33(2)	$\frac{5}{2}^+$ and $\frac{1}{2}$			
	7.414	2.310	0.55(3)	−0.08(3)	$\frac{5}{2}$	$\frac{5}{2}$	1	4
		3.825	0.11(5)	−0.13(6)		$\frac{7}{2}$	1	2
37*b*	7.415	0.0	0.22(6)	−0.05(7)	$\frac{3}{2}^-$	$\frac{5}{2}^-$	1,2	2
		0.237	0.12(6)	−0.21(7)		$\frac{7}{2}^-$	2	5
		1.817	−0.57(5)	−0.05(5)		$\frac{3}{2}$	1,2	1
		1.959	0.08(6)	0.08(6)		$\frac{1}{2}^-$	1,2	2
40	inel.		0.42(2)	−0.09(3)	$\frac{3}{2}^-, \frac{5}{2}^-$			
	7.447	0.0	−0.07(6)	0.00(7)	$\frac{3}{2}^-$	$\frac{5}{2}^-$	1	0.1
		2.276	−0.21(3)	0.06(4)		$\frac{1}{2}^+$	1	3

TABLE IV. (*Continued*).

Resonance No.	E_i (MeV)	E_f (MeV)	A_2	A_4	J_i^π	J_f^π	Multipolarity	χ^2
		2.310	−0.19(6)	−0.13(7)		$\frac{5}{2}^-$	1	5
41	inel.		0.39(4)	−0.06(4)	$\frac{3}{2}^-, \frac{5}{2}^-$			
	7.450	0.0	−0.70(8)	0.14(7)	$\frac{3}{2}^-$	$\frac{5}{2}^-$	1,2	4
		1.825	0.74(6)	0.04(6)		$\frac{3}{2}^-$	1,2	0.6
		2.140	0.74(4)	0.10(4)		$\frac{3}{2}^-$	1,2	7
42	inel.		0.49(2)	−0.54(2)	$\frac{5}{2}^+$			
	7.459	0.237	−0.25(15)	0.12(17)	$\frac{5}{2}$	$\frac{7}{2}^-$	1	6
		1.825	−0.18(5)	−0.20(5)		$\frac{3}{2}^-$	1	5
		2.702	−0.33(5)	−0.16(5)		$\frac{3}{2}^-$	1	4
44	7.467	0.0	0.06(11)	0.17(13)	$\frac{1}{2}^-$	$\frac{5}{2}^-$		2
		1.817	0.08(4)	0.04(4)		$\frac{3}{2}$		2
		2.914	0.02(4)	0.03(4)		$\frac{3}{2}^-$		2
48	inel.		0.51(2)	−0.54(2)	$\frac{5}{2}^+$			
49	inel.		0.31(2)	−0.18(2)	$\frac{5}{2}^-$			
	7.514	0.237	−0.01(3)	−0.10(3)	$\frac{5}{2}^-$	$\frac{7}{2}^-$	1	4
		2.140	−0.24(4)	0.02(5)		$\frac{3}{2}^-$	1	0.6
		2.310	0.26(4)	−0.16(5)		$\frac{5}{2}^-$	1,2	4
		3.049	−0.03(15)	−0.13(16)		$\frac{5}{2}^-$	1,2	3
						$\frac{7}{2}$	1	3
		3.825	0.07(12)	−0.23(13)		$\frac{7}{2}$	1	1.5
52*a*	inel.		0.37(2)	−0.10(2)	$\frac{3}{2}^-, \frac{5}{2}^-$			
	7.529	0.	−0.6(3)	0.05(4)	$\frac{3}{2}^-$	$\frac{5}{2}^-$	1	0.6
		1.959	−1.05(6)	0.07(5)		$\frac{1}{2}^-$	1,2	2
		2.140	0.54(5)	0.01(5)		$\frac{3}{2}^-$	1,2	2
53	7.546	0.0	0.53(4)	0.08(5)	$\frac{5}{2}$	$\frac{5}{2}^-$	1	4
		0.237	−0.11(2)	−0.04(2)		$\frac{7}{2}^-$	1	4
54	inel.		0.11(3)	−0.05(4)	$\frac{1}{2}$			
	7.550	1.825	0.05(6)	0.00(7)	$\frac{1}{2}$	$\frac{3}{2}^-$		1
		2.140	0.04(3)	−0.07(4)		$\frac{3}{2}^-$		4
		2.914	0.08(3)	−0.14(3)		$\frac{3}{2}^-$		3

TABLE IV. (*Continued*).

Resonance No.	E_i (MeV)	E_f (MeV)	A_2	A_4	J_i^π	J_f^π	Multipolarity	χ^2
55	inel.		0.35(2)	−0.10(2)	$\frac{3}{2}^-, \frac{5}{2}^-$			
	7.560	0.	0.33(7)	0.03(8)	$\frac{3}{2}^-, \frac{5}{2}^-, \frac{5}{2}^-$	$\frac{5}{2}^-$	1,2	0.2
		2.140	0.46(4)	0.03(4)		$\frac{3}{2}^-$	1	0.6
		2.256	−0.03(7)	−0.01(7)		$\frac{5}{2}^-$	1	0.1
56	inel.		0.47(8)	−0.50(9)	$\frac{5}{2}^+$			
61	7.618	1.817	0.03(2)	0.06(2)	$\frac{1}{2}$	$\frac{3}{2}^-$		5
		2.140	0.02(10)	−0.01(9)		$\frac{3}{2}^-$		1
		2.276	−0.03(7)	0.02(8)		$\frac{1}{2}^+$		3
62	7.621	0.237	0.11(4)	−0.06(4)	$\frac{9}{2}$	$\frac{7}{2}^-$	1	1
		1.140	0.50(2)	−0.03(2)		$\frac{9}{2}^-$	1	3
		2.416	−0.12(9)	−0.07(9)		$\frac{7}{2}^-$	1	1
63*a*	7.631	0.0	0.49(4)	−0.05(4)	$\frac{5}{2}^-$	$\frac{5}{2}^-$	1	2
		0.237	0.17(2)	0.00(2)		$\frac{7}{2}^-$	1,2	2
		1.140	0.04(11)	0.00(11)		$\frac{9}{2}^-$	2	3
		2.140	−0.25(6)	0.05(6)		$\frac{3}{2}^-$	1	0.6
		2.310	0.46(5)	−0.13(5)		$\frac{5}{2}^-$	1	3
		2.416	0.60(10)	−0.18(10)		$\frac{3}{2}^-$	1	4
		3.049	−0.01(6)	−0.02(6)		$\frac{5}{2}^-$	1	0.2
						$\frac{7}{2}^-$	1,2	0.2
63*b*	inel.		0.49(2)	−0.49(2)	$\frac{5}{2}^+$			
64	inel.		0.54(2)	−0.32(2)	$\frac{5}{2}^-$			
71	inel.		0.41(2)	−0.38(2)	$\frac{5}{2}^+$ and $\frac{1}{2}$			
	7.699	0.0	0.41(5)	−0.14(6)	$\frac{5}{2}$	$\frac{5}{2}^-$	1	6
		0.237	−0.10(8)	−0.02(8)		$\frac{7}{2}^-$	1	0.1
		1.817	−0.50(31)	−0.17(29)		$\frac{3}{2}^-$	1	0.4
		2.310	0.44(17)	0.03(18)		$\frac{5}{2}^-$	1	0.1
72	inel.		0.40(2)	0.06(2)	$\frac{3}{2}^-, \frac{5}{2}^-$			
	7.722	0.0	−0.52(14)	0.06(13)	$\frac{3}{2}^-$	$\frac{5}{2}^-$	1,2	2
		1.825	0.75(27)	0.18(29)		$\frac{3}{2}^-$	1,2	1
		1.959	−0.73(5)	0.07(4)		$\frac{1}{2}^-$	1	2
		2.702	−0.45(15)	0.23(16)		$\frac{3}{2}^-$	1,2	2

tipolarity column indicates those transitions for which the quadrupole-to-dipole intensity ratio exceeds 5%. New assignments for bound states are summarized in Table V where reference to the determining resonances is made. Generally, the analysis of single transitions allowed a number of solutions for an unknown spin, as in the example of Fig. 5. However, the simultaneous fitting to a few primary transitions usually led to a unique spin assignment. In the case of the 2.310 MeV level above, the decay from $R40$, with $J^\pi=\frac{3}{2}^-$, eliminates the $\frac{7}{2}^-$ option, while the decay from $R30$ and $R71$, both spin $\frac{5}{2}$, argues against spin $\frac{3}{2}$ more strongly than does $R49$. In a number of cases, especially for the bound state assignments, restric-

TABLE V. New bound state assignments.

E_x (MeV)	J^π	Resonances	Previous work a	Previous work b
1.817	$\frac{3}{2}^{(-)}$	31,37*b*,71	$(\frac{5}{2})$	$\frac{3}{2}^-$
2.310	$\frac{5}{2}^-$	24*a*,31,40,49	$(\frac{5}{2})$	
2.702	$\frac{3}{2}^-$	31,42,72	$(\frac{3}{2})$	
2.841	$\frac{1}{2},\frac{3}{2}^-$	24*b* and decay	$(\frac{1}{2})^-$	
2.893	$\frac{5}{2}^-$	7,15*b* and decay		
2.985	$\frac{5}{2}$	24*b*,25,32*a* and decay	$(\frac{5}{2})$	$\frac{5}{2}^+$
3.029	$(\frac{7}{2})$	62 only and decay		
3.049	$\frac{5}{2}^-,\frac{7}{2}$	31,49,63 and decay	$(\frac{5}{2},\frac{9}{2})$	$\frac{5}{2}^-,\frac{7}{2}^-$
3.131	$\frac{3}{2}^-,\frac{5}{2}^+$	23*a* and decay	$(\frac{7}{2})$	
3.281	$(\frac{1}{2},\frac{3}{2})$	14*a* only		
3.293	$\frac{5}{2}$	32*b* and decay	$\frac{5}{2}^-,\frac{7}{2}^-$	
3.423	$(\frac{3}{2},\frac{5}{2}^-)$	11,22,63 and decay		
3.554	$(\frac{3}{2})$	1,13,14*b* and decay	$\frac{1}{2}^-,\frac{3}{2}^-$	
3.694	$\frac{3}{2}^-$	24*b* and decay	$\frac{1}{2}^-,\frac{3}{2}^-$	
3.825	$\frac{7}{2}$	27,49 and decay		
3.835	$(\frac{7}{2})$	62 only and decay		
3.877	$(\frac{3}{2},\frac{5}{2})$	63 only and decay		
3.893	$\frac{3}{2}$	24*b* and decay	$\frac{1}{2}^-,\frac{3}{2}^-$	
3.955	$(\frac{7}{2},\frac{9}{2})$	62 only and decay		
4.006	$(\frac{3}{2},\frac{5}{2})$	22,49,55 and decay	$(\frac{1}{2}^+)$	
4.153	$(\frac{5}{2}^+)$	27 only[c] and decay		
4.200	$(\frac{1}{2},\frac{3}{2})$	13,14*a*,19		
4.206	$(\frac{5}{2})$	12,41 and decay		
4.358	$(\frac{3}{2})$	1,9,14*a* and decay		$(\frac{1}{2}^-,\frac{3}{2}^-)$
4.450	$(\frac{3}{2},\frac{5}{2},\frac{7}{2})$	15*b*,23	$(\frac{7}{2})^-$	
4.488	$(\frac{5}{2})$	24,41,55		$\frac{5}{2}^-,\frac{7}{2}^-$
4.540	$(\frac{3}{2},\frac{5}{2},\frac{7}{2})$	23*a*,24*a*,37		
4.729	$(\frac{1}{2},\frac{3}{2})$	13,32*b*		
4.883	$\frac{1}{2},\frac{3}{2}^-$	25,44 and decay		
5.067	$(\frac{3}{2})$	32*b* only and decay		
5.074	$(\frac{1}{2},\frac{3}{2},\frac{5}{2})$	16 only	$\frac{1}{2}^-,\frac{3}{2}^-$	
5.129	$(\frac{3}{2},\frac{5}{2})$	16,56 and decay	$\frac{1}{2}^-,\frac{3}{2}^-$	
5.174	$(\frac{1}{2},\frac{3}{2},\frac{5}{2})$	25,65	$(\frac{3}{2}^+,\frac{5}{2}^+)$	

[a]Reference 1.
[b]Reference 5.
[c]Seen also in the decay of the $g_{9/2}$ isobaric analog states, Ref. 32.

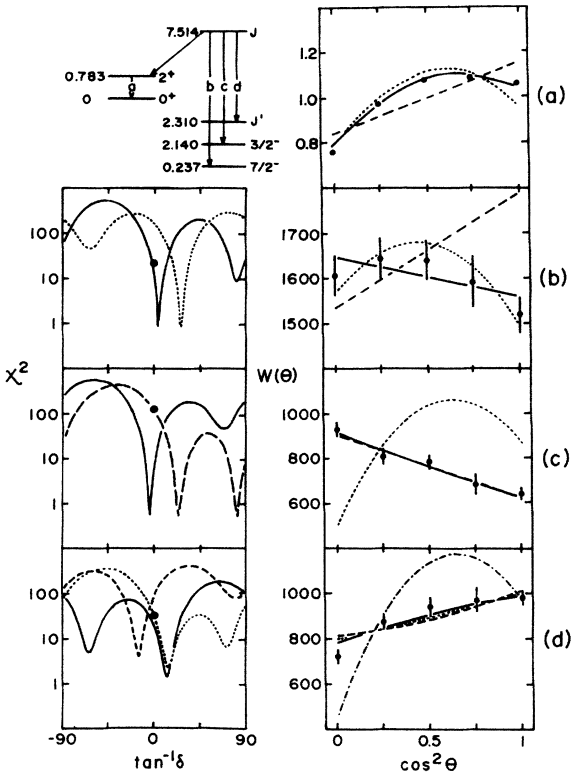

FIG. 5. Angular distributions in the decay of $R49$, at $E_p=2.288$ MeV, and their analysis. (a) $(p,p'\gamma)$; (b) (p,γ), $R49\rightarrow 0.237$ MeV, $J\rightarrow\frac{7}{2}$; (c) (p,γ) $R49\rightarrow 2.140$ MeV, $J\rightarrow\frac{3}{2}$; (d) (p,γ) $R49\rightarrow 2.310$ MeV, $\frac{5}{2}\rightarrow J'$. J and J' are denoted by $\frac{1}{2}$, dot-dash line; $\frac{3}{2}$, dashed; $\frac{5}{2}$, solid; $\frac{7}{2}$, dotted. The solid points in the χ^2 vs $\tan^{-1}\delta$ graphs are for $J=\frac{3}{2}$ and $\frac{7}{2}$ in (b) and (c), respectively, and $J'=\frac{1}{2}$ in (d).

tion or removal of ambiguities was helped by considering secondary branching. For instance, the 79% branch from the 2.310 MeV level to the $\frac{7}{2}^-$ 0.237 MeV level strongly favors the $\frac{5}{2}^-$ assignment, rather than $\frac{3}{2}^-$.

IV. DISCUSSION

A. Resonance properties

The only yield curve previously measured for the $^{50}Cr(p,\gamma)^{51}Mn$ reaction is given by Arnell[12] who measured up to 2 MeV. The resonance energies agree well in the overlap region. There are measurements of the excitation function for elastic scattering above 1.8 MeV. The 68 resonances found in the present study from 1.8 to 2.5 MeV may be compared to the 25 reported by Moses *et al.*[26] There is a consistent discrepancy of about 5 keV between corresponding resonances in the higher precision elastic scattering experiments and the radiative capture. The former experiments are insensitive at such low proton energies to resonances of higher angular momentum, whereas capture and inelastic scattering are weaker at s-wave resonances.

There is fairly good consistency between spin-parity assignments based on capture and inelastic scattering angular distributions. Where there is not, it is likely that multiple unresolved resonances exist. This was confirmed in some instances by careful yield curve measurements. The results agree well with those of others. For instance, resonances 1 and 5 were assigned in the (p,γ) work of Erlandsson[16] as having spin $\frac{3}{2}$ or $\frac{5}{2}$, with a preference for $\frac{3}{2}$. Din and Al-Naser assigned spin $\frac{5}{2}$ to resonances 24 and 25 in their work.[22] As has been noted above, the elastic scattering experiments below 3 MeV detected only s and p resonances clearly. The present spin results are in fairly good agreement with those of Moses *et al.*[26] and Dittrich *et al.*[27] The one resonance below 2.5 MeV assigned as $l>1$ ($\frac{5}{2}^+$) by Moses *et al.* at 2.340 MeV is confirmed in this work (resonance 56). There are a few spin and parity discrepancies, however, which bear on the selection of isobaric analog states.

B. Isobaric analog resonances

With a fairly comprehensive set of energy, spin, and parity assignments for the resonances in ^{51}Mn up to 2.5 MeV ($E_x=7.7$ MeV), it is possible to try to complete the list of suggested analogs of ^{51}Cr in this energy range. (See Table VI.) The levels of the latter are well documented up to $E_x=3.2$ MeV, primarily from (d,p) and (n,γ) experiments on ^{50}Cr and $^{48}Ti(\alpha,n\gamma)$.[1,38,39] The analogs of the lowest three states of ^{51}Cr fall among the bound states of ^{51}Mn and are discussed below. The next three levels have spin $\frac{9}{2}^-$, $\frac{5}{2}^-$, and $\frac{7}{2}^-$ and would form very weak resonances at such a low energy. The first clear analog resonance is at $E_p=1.059$ MeV and has been thoroughly studied.[18–20] Above this are three more $l=3$ levels in ^{51}Cr. The first two may have analogs among the resonances whose spectra were studied by Forsblom *et al.*[19] but no spin or proton widths are available. The present study addresses the next 13 states of ^{51}Cr, from 2.7 to 3.2 MeV (omitting levels of high spin). For most of the ^{51}Cr levels, a number of resonances allow interpretation as analogs. The only exception to spin-parity agreement appears to be at 1.943 MeV ($E_x=7.176$ MeV) for which the present experiment yields $J^\pi=\frac{5}{2}^+$. Moses *et al.*[26] reported a $\frac{1}{2}^+$ level there which may form an undetected doublet with the resonance observed in this work.

The Coulomb energy shift ΔE_C was calculated for each proposed analog pair according to

$$\Delta E_C=E_x(\mathrm{Mn})-E_x(\mathrm{Cr})+Q(\mathrm{Mn}\rightarrow\mathrm{Cr})+Q(\mathrm{n}\rightarrow\mathrm{H})\ .$$

It may be seen that it remains quite constant near 8.40 MeV throughout the full range of excitation energies. The only notable exception is the $\frac{1}{2}^-$ 0.777 MeV level of ^{51}Cr. The above value of ΔE_C may be compared with that at the $d_{5/2}$ and $g_{9/2}$ analogs at $E_x=3.97$ and 4.15 MeV in Cr, which are 8.37 and 8.30 MeV, respectively.

Many of the resonances which are analog state candidates show strong transitions to only one or two bound levels. Examples are resonance 31 at 2.118 MeV which decays primarily (69%) to the 2.702 MeV level, and resonance 35 at 2.167 MeV which decays only to the ground (38%) and 3.292 MeV state (62%).

TABLE VI. Proposed isobaric analog states in ^{51}Cr-^{51}Mn.

^{51}Cr			^{51}Mn			
E_x (MeV)	J^π a,b	Resonance No.	E_x (MeV)	J^π c		ΔE_c (MeV)
0.0	$\frac{7}{2}^-$		4.450	$\frac{7}{2}^-$	d	8.402
0.749	$\frac{3}{2}^-$		5.125	$\frac{3}{2}^-$	d	8.368
0.777	$\frac{1}{2}^-$		5.074	$\frac{1}{2}^-$	d	8.289
⋮			⋮			
1.899	$\frac{3}{2}^-$		6.309	$\frac{3}{2}^-$	e	8.402
⋮			⋮			
2.704	$(\frac{7}{2}^-)$	7	7.106	$\frac{5}{2}^-, \frac{7}{2}^-$		8.394
		11	7.141	$(\frac{7}{2})$		8.429
2.763	$\frac{1}{2}^+$	15*b*	7.176	$\frac{1}{2}^+$	f	8.405
⋮			⋮			
2.829	$\frac{3}{2}^-$	24*b*	7.274	$\frac{3}{2}^-$		8.435
		25	7.296	$\frac{3}{2}^-$		8.457
2.890	$\frac{3}{2}^-$	28	7.314	$(\frac{1}{2}, \frac{3}{2})$		8.416
		29	7.339	$(\frac{1}{2}, \frac{3}{2})$		8.441
		30*b*	7.343	$\frac{3}{2}^-$	f	8.443
2.911	$\frac{5}{2}^-$	31	7.357	$\frac{5}{2}^-$		8.436
2.949	$\frac{5}{2}^-$	35	7.395	$\frac{3}{2}^-, \frac{5}{2}^-$		8.436
2.970	$(\frac{3}{2}^+)$	37*a*	7.415	$\frac{5}{2}^+$		8.435
3.002	$\frac{3}{2}^-, \frac{5}{2}^-$	40	7.447	$\frac{3}{2}^-$		8.435
3.004	$(\frac{5}{2})^-$	41	7.450	$\frac{3}{2}^-$		8.435
3.020	$(\frac{3}{2})^+$	42	7.459	$\frac{5}{2}^+$		8.429
3.055	$(\frac{1}{2})^-$	44	7.467	$\frac{1}{2}^-$		8.402
3.109		55	7.560	$\frac{3}{2}^-, \frac{5}{2}^-$		8.441
3.135	$\frac{3}{2}^-$	58	7.586	$\frac{1}{2}, \frac{3}{2}$		8.441
3.207	$\frac{7}{2}^-$	67	7.669	$(\frac{5}{2}, \frac{7}{2})$		8.452

[a]Reference 1.
[b]References 38 and 39.
[c]Present work, except as noted.
[d]Reference 3, see the text, Sec. IV C.
[e]References 18–20.
[f]References 26 and 27.

C. Bound states

Most of the previous information on the decays of bound levels of ^{51}Mn comes from (p,γ) (Refs. 19 and 22) and (p,$\alpha\gamma$) (Ref. 9) reactions. Forsblom *et al.*[19] reported the decay schemes of bound levels from the study of 19 resonances below 1.7 MeV while the results of Din and Al-Naser[22] were from the investigation of ten resonances below 2.1 MeV. In the present study, the capture spectra and angular distributions have revealed a few new bound levels in ^{51}Mn and refined data on many others as indicated in Tables III and V. There is general agreement with the previous results for some of the bound levels with only small differences in decay branching. There are a number of others in which more significant differences with the earlier work appear. For instance, the decay of the 2.276 MeV level differs from that given by Forsblom *et al.*[19] and Noé *et al.*[9] The 82% feeding from resonance 29 at 2.110 MeV gave a clear spectrum to determine the cascades, so five branches, with energies down to 0.136 MeV, could be seen. The levels at 2.310 and 2.702 MeV were most clearly seen at the 2.128 MeV resonance (No. 31) with a 69% decay branch to the 2.702 MeV state followed by a 38% cascade to the 2.310 MeV state. The decay scheme of the 3.049 MeV level differs from that given by Forsblom *et al.* and Din and Al-Naser. Park *et al.*[5] reported a doublet at this energy so the state found in this work may not be the same as the one seen previously. A particularly significant revision is that of the decay scheme of the 4.450 MeV level, the supposed analog of

the ^{51}Cr ground state ($\frac{7}{2}^-$). The strong branch to the $\frac{1}{2}^-$ 1.959 MeV level reported by Din and Al-Naser was not confirmed in the present work.

The spin-parity determinations indicated in Table V cast light on previous interpretations of parts of the spectrum of ^{51}Mn. The first several levels listed form a group for which parity information has been lacking. This led Noé *et al.*[9] to propose the existence of two coupled positive parity bands (1.817, 2.310, 2.893 MeV; $K^\pi=\frac{3}{2}^+$) and (2.276, 2.702, 2.985 MeV: $K^\pi=\frac{3}{2}^+$). The authors do note that the preponderance of out-of-band transitions is a difficulty with this interpretation. The angular distribution data presented here confirm the spins used by Noé *et al.* but the existence of appreciable dipole-quadrupole mixing from negative-parity resonances seems to require negative parity for the 1.817, 2.310, 2.702, and 2.893 MeV levels. The positive parities of the 2.276 and 2.985 MeV levels from $l=0$ and $l=2$ (^{3}He,d) transfers[3,5] are consistent with the present work.

With a few exceptions, the remaining assignments are consistent with earlier, less restrictive determinations. Most of the levels were observed at many resonances, though only those pertinent to the spin-parity determinations are listed in Table V. Those few that were seen at only one resonance have also been seen by others, as indicated in the table. Four levels of some interest in this regard are the three (3.029, 3.835, 3.955 MeV) fed only from the $\frac{9}{2}^+$ $E_p=2.397$ MeV resonance, No. 62, and one (4.153 MeV) fed from the $\frac{9}{2}^+$ analog state at $E_p=3.2$ MeV.[32] All are moderately high in spin, but only one, the level at 3.955 MeV, could be $\frac{9}{2}^+$ and therefore a nominee as the $g_{9/2}$ antianalog state. This level is not fed from the analog state, nor is it seen in (^{3}He,d), two failings which seem to disqualify its candidature.

Three bound levels observed strongly in (^{3}He,d) and proposed as the isobaric analogs of the lowest three states of ^{51}Cr are at 4.451, 5.077, and 5.125 MeV. The present spin restrictions of the three are consistent with the requirements $\frac{7}{2}^-$, $\frac{1}{2}^-$, and $\frac{3}{2}^-$. The inversion between parent and analog of the close-lying $\frac{1}{2}^-$ and $\frac{3}{2}^-$ states is not unprecedented.

Park *et al.*[5] reported a doublet at 3.426 MeV. Our observation at 3.426 MeV agrees with the level seen in (p,α) and may differ from the 3.423 MeV level seen in earlier (p,γ) experiments. In addition to the known level at 4.206 MeV, there is a new level at 4.200 MeV.

Shell model calculations of the $T=\frac{1}{2}$ states of ^{51}Mn are formidable in any space other than an $f_{7/2}^{11}$ basis. Matrices of dimension $\sim 10^3$ can occur when the upper fp shell is opened. Calculations confined to the $f_{7/2}$ shell do not predict any $\frac{1}{2}^-$ or $\frac{3}{2}^-$ levels below 2.5 or 3 MeV so the low-spin negative-parity states near 2 MeV must surely arise from fp excitations. This is supported by the large (^{3}He,d) spectroscopic factors to the 1.825 and 1.959 MeV levels.[3,5] Calculations restricted to the $f_{7/2}^{11}$, $f_{7/2}^{10}p^1$, and $f_{7/2}^{9}p^2$ configurations do bring low spin states down to below 2 MeV,[40,41] suggesting that more extensive calculations may be successful in reproducing the entire negative parity structure observed, including the difference in character between the two members of the $\frac{3}{2}^-$ doublet at 1.82 MeV.

V. CONCLUSIONS

In the present high resolution investigation, the decay properties of a large number of resonances in ^{51}Mn have been found. A considerable addition has been made to the available information about the bound states, for which revised decay schemes and spin-parity measurements are offered. Thirteen candidate analog states are proposed.

ACKNOWLEDGMENTS

The authors wish to acknowledge the considerable assistance of Hassan Khadr in operating the King Saud Van de Graaff and of James Stark at the McMaster accelerator. Special runs of the shell model code by A. A. Pilt are greatly appreciated. The work was financially supported by the Natural Sciences and Engineering Research Council of Canada and the Research Council of the Faculty of Sciences, King Saud University.

[1]R. L. Auble, Nucl. Data Sheets **23**, 163 (1978).
[2]L. Nilsson and B. Erlandsson, Z. Phys. **232**, 303 (1970).
[3]J. Rapaport, T. A. Belote, and W. E. Dorenbusch, Nucl. Phys. **A100**, 280 (1967).
[4]N. Nakanishi, S. Takeda, H. Ohnuma, S. Yamada, H. Sakaguchi, M. Nakamura, S. Takeuchi, and K. Koyama, Institute of Physics and Chemical Research, RIKEN Progress Report No. 8, 1974, p. 48.
[5]J. E. Park, W. W. Daehnick, and M. J. Spisak, Phys. Rev. C **19**, 42 (1979).
[6]T. Matsuzaki, M. Adachi, and H. Taketani, J. Phys. Soc. Jpn. **43**, 369 (1977).
[7]J. E. Kim and W. W. Daehnick, Phys. Rev. C **23**, 742 (1981).
[8]R. W. Tarara, J. D. Goss, P. L. Jolivette, G. F. Neale, and C. P. Browne, Phys. Rev. C **13**, 109 (1976).
[9]J. W. Noé, R. W. Zurmühle, and D. P. Balamuth, Nucl. Phys. **A277**, 137 (1977).
[10]Y. Tagishi, K. Katori, Y. Toba, and M. Sasagasi, J. Phys. Soc. Jpn. **47**, 1735 (1979).
[11]G. Fortuna, S. Lunardi, M. Morando, and C. Signorini, Nucl. Phys. **A299**, 479 (1978).
[12]S. E. Arnell, Ark. Fys. **21**, 177 (1961).
[13]S. E. Arnell and S. Sterner, Ark. Fys. **26**, 309 (1964).
[14]S. Sterner, L. Jonsson, and S. E. Arnell, Ark. Fys. **31**, 567 (1966).
[15]M. A. Abuzeid, M. I. El-Zaiki, N. A. Mansour, A. I. Popov, H. R. Saad, and V. E. Stroizhko, Z. Phys. **199**, 506 (1967).
[16]B. Erlandsson, Ark. Fys. **34**, 285 (1967).
[17]N. Wall and B. Erlandsson, Ark. Fys. **34**, 325 (1967).
[18]H. V. Klapdor, Phys. Lett. **35B**, 405 (1971).
[19]I. Forsblom, T. Weckström, T. Sundius, G. Bergström, S. Forss, and G. Wansén, Phys. Scr. **6**, 309 (1972).

[20]M. Schrader, K. Bucholz, and H. V. Klapdor, Nucl. Phys. **A223**, 365 (1974).
[21]B. A. Nemashkalo, O. I. Ekhichev, A. P. Klyucharev, G. A. Krivonosov, A. I. Popov, V. E. Storizhko, and V. K. Chirt, Yad. Fiz. **19**, 1185 (1974) [Sov. J. Nucl. Phys. **19**, 605 (1975)].
[22]G. U. Din and A. M. Al-Naser, Aust. J. Phys. **28**, 263 (1978).
[23]A. E. Antropov, V. P. Gusov, P. P. Zarubin, and P. D. Ionnu, Probl. Yad. Fiz. Kosm. Luchei **8**, 18 (1978).
[24]A. Brondi, R. Moro, V. Roca, F. Terrasi, and B. Gonsior, Lett. Nuovo Cimento **33**, 25 (1982).
[25]G. C. Kyker, Jr., E. G. Bilpuch, and H. W. Newson, Ann. Phys. (N.Y.) **51**, 124 (1969).
[26]J. D. Moses, E. G. Bilpuch, H. W. Newson, and G. E. Mitchell, Nucl. Phys. **A175**, 556 (1971).
[27]T. R. Dittrich, C. R. Gould, G. E. Mitchell, E. G. Bilpuch, and K. Stelzer, Nucl. Phys. **A279**, 430 (1977).
[28]M. Salzmann, V. Meyer, and H. Brandle, Nucl. Phys. **A282**, 317 (1977).
[29]E. Arai, M. Futakuchi, J. Komaki, M. Ogawa, and Y. Oguri, J. Phys. Soc. Jpn. **52**, 802 (1983).
[30]J. F. Shriner, Jr., K. M. Whatley, E. G. Bilpuch, C. R. Westerfeldt, and G. E. Mitchell, Z. Phys. A **313**, 51 (1983).
[31]K. M. Whatley, E. G. Bilpuch, G. E. Mitchell, and J. F. Shriner, Jr., J. Phys. G **9**, 1527 (1983).
[32]J. Sziklai, J. A. Cameron, and I. M. Szöghy, Phys. Rev. C **30**, 490 (1984).
[33]W. Kutschera, B. A. Brown, and K. Ogawa, Riv. Nuovo Cimento **1**, No. 12 (1978).
[34]G. U. Din, A. M. AlSoraya, J. A. Cameron, and J. Sziklai, Phys. Rev. C **31**, 1366 (1985).
[35]G. U. Din, J. A. Cameron, V. P. Janzen, and R. B. Schubank, Phys. Rev. C **31**, 800 (1985).
[36]H. J. Rose and D. M. Brink, Rev. Mod. Phys. **39**, 306 (1967).
[37]C. van der Leun and G. J. L. Nooren, Phys. Lett. **98B**, 26 (1981).
[38]J. Kasagi and H. Ohnuma, J. Phys. Soc. Jpn. **45**, 1099 (1978).
[39]J. Kasagi and H. Ohnuma, J. Phys. Soc. Jpn. **48**, 351 (1980).
[40]A. Yokoyama and H. Horie, Phys. Rev. C **31**, 1012 (1985).
[41]A. A. Pilt, private communication.